2024 IEEE 35th International Symposium on Personal, Indoor and Mobile Radio Communications (PIMRC) | 979-8-3503-6224-4/24/$31.00 ©2024 IEEE | DOI: 10.1109/PIMRC59610.2024.10817175

Energy-Aware Trajectory Design for UAV-mounted Full-duplex Relays

Dimitrios Tyrovolas*†, Nikos Mitsiou*, Thomas Boufikos*, Sotiris Tegos* Prodromos-Vasileios Mekikis‡, Panagiotis Diamantoulakis*, Sotiris Ioannidis†, Christos Liaskos§, George Karagiannidis*¶
*Department of Electrical and Computer Engineering, Aristotle University of Thessaloniki, 54124 Thessaloniki, Greece
e-mail: {tyrovolas, nmitsiou, mpothogeo, tegosoti, padiaman, geokarag}@auth.gr
†Dept. of Electrical and Computer Engineering, Technical University of Crete, Chania, Greece, e-mail: sotiris@ece.tuc.gr
‡Hilti Corporation, Feldkircher Strasse 100, 9494 Schaan, Liechtenstein, e-mail: akis.mekikis@hilti.com
§Computer Science Engineering Department, University of Ioannina, Ioannina, Greece. e-mail: cliaskos@ics.forth.gr
¶Artificial Intelligence & Cyber Systems Research Center, Lebanese American University (LAU), Lebanon

***Abstract*—Unmanned aerial vehicles (UAVs) equipped with full-duplex relays (FDRs) are pivotal in overcoming connectivity challenges by dynamically establishing effective communication channels. However, despite their potential in network performance via trajectory optimization, integrating energy consumption models for UAV-mounted FDRs remains unexplored, crucial for trajectory design adhering to existing energy constraints. To this end, we introduce an energy-aware trajectory optimization framework to maximize network performance and user fairness within the UAV's energy constraints. Specifically, we present a detailed energy consumption model describing the operational needs of UAV-mounted FDRs and formulate a joint time-division multiple access (TDMA) user scheduling-UAV trajectory optimization problem considering the power dynamics of UAV-mounted FDRs. Finally, our simulation results highlight the role of energy awareness in achieving optimal trajectory and scheduling, contributing to UAV-mounted FDRs' performance in future networks.**

***Index Terms*—Unmanned aerial vehicles (UAVs), full-duplex relays, trajectory optimization, energy efficiency, energy awareness**

I. Introduction

Over the last few years, unmanned aerial vehicles (UAVs) have been envisioned as key components of future wireless networks that can offer ubiquitous line-of-sight (LoS) channels by dynamically adjusting their paths [1], [2]. However, despite these advantages, UAVs face the challenge of limited on-board energy, which constrains their operational time [3], underscoring the need to maximize their operational efficiency within their flight duration. In this direction, the integration of full-duplex relays (FDRs) with UAVs, namely UAV-mounted FDRs, introduces a novel approach for enhanced spectral efficiency due to their ability for simultaneous data transmission and reception [4]. Specifically, UAV-mounted FDRs can optimally use the available time slots during the UAV flight, while also offering resilience against path loss, making them a strong candidate for maintaining robust communication links. Therefore, understanding the advantages and challenges of UAV-based FDRs becomes essential in shaping future networks.

The integration of UAV-mounted FDRs with wireless networks is a promising research direction. [5] showcased the robust capabilities of UAV-mounted FDRs for real-time data exchange and path loss mitigation, while [6] emphasized the critical role of precise UAV trajectory planning in optimizing network performance. Additionally, [7] explored millimeter-wave scenarios, highlighting the adaptability of UAV-mounted FDRs to high-frequency challenges and the importance of trajectory optimization in overcoming communication barriers. However, integrating energy-aware trajectory optimization within UAV-mounted FDR systems, crucial for their sustainable and efficient deployment, remains underexplored. Most existing works develop algorithms focusing on trajectory, user scheduling, and power optimization, but they exclude practical energy consumption models and appropriate energy-aware constraints, risking infeasible trajectories that exceed UAV energy limitations [4], [8]. This challenge is intensified by FDR tasks like decoding and self-interference (SI) mitigation, which increase energy usage [9]. Additionally, path loss characteristics introduce uncertainty in UAV energy consumption, as navigating to optimize path loss across various locations complicates energy management. Thus, to the best of our knowledge, no work thoroughly integrates energy consumption models with trajectory optimization for UAV-mounted FDRs to ensure enhanced network performance that adheres to UAV energy limitations.

In this work, we optimize UAV-mounted FDR systems by introducing accurate energy consumption models that capture the relationship between flight duration and UAV operational needs. Specifically, our approach proposes a joint optimization framework for TDMA user scheduling and UAV trajectory, tailored to the specific power dynamics of UAV-mounted FDRs, aiming to enhance the minimum data rate across the network while ensuring user fairness and operational feasibility within the UAV's energy constraints. Moreover, through our simulation results, we demonstrate the significant impact of strategic trajectory planning and energy-aware design principles on network performance. Specifically, our results show how optimized user scheduling and UAV trajectory can substantially improve user fairness and network performance, while underscoring the essential role of optimizing UAV flight paths within energy constraints. Consequently, our work contributes to the practical and efficient deployment of UAV-mounted FDRs in future 6G networks by highlighting the importance of integrating energy awareness into the UAV trajectory optimization

979-8-3503-6224-4/24/$31.00 ©2024 IEEE

process.

II. System Model

We examine a network comprising K ground nodes (GNs) distributed randomly across a rectangular region with sides L, alongside a base station (BS) that additionally functions as a UAV charging station (CS). Given the challenging propagation conditions marked by excessive distances, physical obstructions, and the limited transmission power of the GNs, it is assumed that direct communication links between the GNs and the BS are unfeasible. To mitigate this, a rotary-wing UAV equipped with an FDR serves as a relaying node, facilitating LoS communication between the GNs and the BS by navigating a predetermined trajectory before returning to the BS for recharging [10]. Finally, it is imperative to ensure that the communication equipment is mounted on the UAV in a manner that does not disrupt the airflow around its motors, thus preserving its aerodynamic stability [11].

Considering a 3D Cartesian coordinate system, we assume that the rectangular region's center coincides with the origin of the coordinate system, the BS location is equal to $\boldsymbol{l_{BS}} = [0, 0, H_{\rm BS}]$, where $H_{\rm BS}$ represents the BS height, the UAV flies at a fixed altitude H_u, and the K GNs are located at $\boldsymbol{l_k} = [x_k, y_k, 0]$, where $k \in \{1, \ldots, K\}$, respectively. Furthermore, considering that the trajectory duration equals to T, the UAV location at time t can be written as $\boldsymbol{q}(t) = [x_q(t), y_q(t), H_u]$, where $0 \leq t \leq T$ and $(x_q(t), y_q(t))$ denote the x-y UAV coordinate at time t. However, for tractability reasons, the flight duration T is divided into N equal time slots, i.e., $T = N\delta_t$, where δ_t is the duration of each time slot. Hence, the UAV trajectory $\boldsymbol{q}(t)$ during T can be efficiently approximated by a N-length sequence $\boldsymbol{q}_{[n]} = [x_{q[n]}, y_{q[n]}, H_u]$, $n \in \mathcal{N}, \mathcal{N} = \{1, \ldots, N\}$, where $\left(x_{q[n]}, y_{q[n]}\right)$ denote the x-y UAV coordinate at n-th time slot. Finally, the total number of time slots N is derived considering the UAV battery capacity B_c and its average power consumption per slot $\tilde{P}$, calculated as $N = \left\lfloor \frac{B_c}{\tilde{P}} \right\rfloor$.

A. Achievable Rate

A UAV-mounted FDR with $A_n = A_r + A_t$ antennas can provide improved spectral efficiency because it can simultaneously use A_r antennas for reception and A_t antennas for transmission within a time slot. It is important to note, however, that FDRs are inherently susceptible to SI, highlighting the importance of advanced SI suppression techniques to enable their successful operation [4]. To this end, assuming that the UAV-mounted FDR employs the DF protocol and that A_r antennas perform maximum ratio combining (MRC) and A_t antennas perform maximum ratio transmission (MRT) [12], the achievable rate of the k-th GN within the n-th time slot can be expressed as $R_{\rm k[n]} = \min\left(R_{1[n]}, R_{2[n]}\right)$, where $R_{1[n]}$ denotes the achievable rate from the k-th GN to the UAV-mounted FDR at the n-th time slot, and $R_{2[n]}$ denotes the achievable rate from the UAV-mounted FDR to the BS at the n-th time slot, and can be described as

$$R_{1[n]} = Ba_{k[n]} \log_2\left(1 + \frac{P_t \ell_{1[n]} G_t A_r}{A_t G_r P_{u[n]} \omega + {\sigma_1}^2}\right), \tag{1}$$

and

$$R_{2[n]} = Ba_{k[n]} \log_2\left(1 + \frac{A_t G_r P_{u[n]} \ell_{2[n]}}{\sigma_2^2}\right), \tag{2}$$

where $P_{u[n]}$ is the FDR transmit power at the n-th time slot, $\sigma_1^2 = \sigma_2^2 = \sigma^2$ denote the variance of the AWGN affecting the FDR and the BS, respectively, and $\omega \in [0, 1]$ is the self-interference cancellation (SIC) coefficient. Moreover, $\ell_{1[n]}$ and $\ell_{2[n]}$ describe the path loss of the GN-FDR and the FDR-BS links, respectively, and are expressed as $\ell_{i[n]} = C_0 \left(\frac{d_0}{d_{i[n]}}\right)^{n_p}$, where $i \in \{1, 2\}$, n_p is the path-loss exponent, $C_0 = \left(\frac{\lambda}{4\pi}\right)^2$ is the path loss at the reference distance d_0 with λ denoting the wavelength, while $d_{1[n]}$ and $d_{2[n]}$ express the distances of the GN-FDR and the FDR-BS links at the n-th time slot, respectively, and are equal to $d_{1[n]} = \|\boldsymbol{q}_{[n]} - \boldsymbol{l_{k[n]}}\|$, and $d_{2[n]} = \|\boldsymbol{l_{BS}}_{[n]} - \boldsymbol{q}_{[n]}\|$, with $\|\cdot\|$ being the Euclidean norm. Finally, considering the LoS nature of air-to-ground communication links, i.e., $n_p = 2$, then $R_{1[n]}$ and $R_{2[n]}$ can be rewritten as

$$R_{1[n]} = Ba_{k[n]} \log_2\left(1 + \underbrace{\frac{P_t C_0 {d_0}^2 G_t A_r}{{d_{1[n]}}^2 \left(A_t G_r P_{u[n]} \omega + \sigma^2\right)}}_{\gamma_{1[n]}}\right), \tag{3}$$

and

$$R_{2[n]} = Ba_{k[n]} \log_2\left(1 + \underbrace{\frac{A_t G_r P_{u[n]} C_0 {d_0}^2}{{d_{2[n]}}^2 \sigma^2}}_{\gamma_{2[n]}}\right). \tag{4}$$

In addition, the SNR at the receiver side for the UAV-mounted FDR case when the k-th GN is served is equal to $\gamma_{r,k[n]} = \min\left(\gamma_{1[n]}, \gamma_{2[n]}\right)$. Finally, it should be mentioned that we assume that the GNs transmission power $P_{t[n]}$ is constant within the UAV flight, i.e., $P_{t[n]} = P_t$.

Remark 1: By setting $\gamma_{1[n]} = \gamma_{2[n]}$ we can derive the optimal FDR transmission power that maximizes the achievable rate of the k-th GN at the n-th time slot, which is given as

$$P_{u[n]}^* = \frac{-d_{1[n]}\sigma^2 + \sigma\sqrt{{d_{1[n]}}^2\sigma^2 + 4\omega P_t {d_{2[n]}}^2 G_t A_r}}{2A_t G_r \omega d_{1[n]}}. \tag{5}$$

B. UAV Power Consumption

Understanding the power dynamics of UAVs, especially when integrating different communication technologies, is critical given the inherent battery constraints of UAVs that result in finite flight duration. Specifically, the power consumption of a UAV-mounted FDR can be described as

$$P_{d[n]} = P_{\rm th[n]} + P_{\rm c} + P_{\rm tr}, \tag{6}$$

where $P_{\rm th[n]}$ refers to UAV thrusting and encompasses the power demands for transitioning, countering wind drag, and

related activities. In addition, $P_{\rm c}$ denotes the power required by the FDR, while $P_{\rm tr}$ is a minimal constant power associated with the UAV navigational communication and can be regarded as negligible. To elaborate further on the required power for the consumption model, the power consumption for the FDR operation $P_{\rm c}$ is given as $P_{\rm c} = P^{*}_{u[n]}\,(1+\alpha) + A_n P^{C}_{R}$, where α is the inverse of the power amplifier drain efficiency, and P^{C}_{R} denotes the power consumption of an A_n-antenna transceiver which encompasses the mixer power, the power of phase shifters for each antenna during transmission and reception, the power of each low-noise amplifier per antenna, the frequency synthesizer power, and the encoder power consumption [13].

Considering the inherent dynamics of UAVs, the thrusting power $P_{\rm th}$ plays a pivotal role in the total power consumption. Notably, $P_{\rm th}$ varies within each time slot, being greatly affected by the UAV speed, weight, aerodynamic design, and other on-board components such as the battery weight. Thus, regarding the consumption model presented in [14], $P_{{\rm th}[n]}$ can be reliably characterized as $P_{{\rm th}[n]} = C_1 W^2_{[n]} + C_2 W_{[n]} + C_3$, where C_1, C_2, and C_3 are motor-dependent parameters, while $W_{[n]}$ encompasses all weight components impacting thrusting power, which can be expressed as $W_{[n]} = U_{\rm w} + D_{\rm w} + R_{\rm w} + S_{{\rm w}[n]}$. In more detail, $U_{\rm w}$ expresses the weight of the UAV frame and its battery, while $D_{\rm w} = \frac{\rho_a v_a^2 C_d A_{\rm UAV}}{2g}$ describes the wind drag, where ρ_a is the air density, g is the gravity acceleration, v_a is the average wind velocity, C_d is the drag shape coefficient given experimentally, and $A_{\rm UAV}$ is the UAV frame area. Moreover, $R_{\rm w}$ is the FDR weight, where for an FDR with A_n antennas is equal to $R_{\rm w} = A_n A_{\rm w}$, where $A_{\rm w}$ is the weight of each FDR antenna, respectively. Finally, $S_{{\rm w}[n]}$ is the extra weight added to the motors due to any change in the speed of the UAV in each time slot.

$$S_{{\rm w}[n]} = (T_{\max} - U_{\rm w} - D_{\rm w} - R_{\rm w})\frac{\upsilon_{[n]}}{\upsilon_{\max}}, \tag{7}$$

with $T_{\max}$ being the maximum achievable thrust, $\upsilon_{[n]} = \frac{\|\boldsymbol{q}_{[n]} - \boldsymbol{q}_{[n-1]}\|}{\delta_t}$ reflecting the average UAV speed within the n-th time slot, and $\upsilon_{\max}$ expressing the maximum achievable UAV speed. Finally, considering (1) and the available B_c, by setting $\upsilon_{[n]} = 0$ or $\upsilon_{[n]} = \upsilon_{\max}$ in (20), we can obtain the maximum and the minimum flight duration in terms of time slots.

III. Energy-Aware Trajectory Design

A. Problem Formulation

To efficiently maximize the minimum data rate of the network, we aim to jointly optimize the UAV trajectory and TDMA user scheduling, taking into account mobility, user scheduling, and UAV power consumption constraints. Given these considerations, by leveraging the integer variable $\boldsymbol{A}$ that represents the TDMA scheduling, and the continuous variable $\boldsymbol{Q}$ that describes the UAV trajectory, the optimization problem for the examined scenario can be formulated as

$$\begin{aligned}
&\max_{\boldsymbol{A},\boldsymbol{Q}} \min_{k} \left\{ \sum_{n=1}^{N} R_{k[n]} \right\} \\
\textbf{s.t}\ \ &\mathrm{C}_1: \boldsymbol{q}_{[1]} = \boldsymbol{q}_{[N]}, \\
&\mathrm{C}_2: \upsilon_{[n]} \le \upsilon_{\max},\ \forall n \in \mathcal{N}, \\
&\mathrm{C}_3: \sum_{k=1}^{K} a_{k[n]} \le 1,\ \forall n \in \mathcal{N}, \\
&\mathrm{C}_4: B_c - \delta_t \sum_{n=1}^{N} P_{d[n]} \ge 0, \\
&\mathrm{C}_5: a_{k[n]} \in \{0,1\},\ \forall n \in \mathcal{N}, \\
&\mathrm{C}_6: q_{\min} \le \boldsymbol{q}_{[n]} \le q_{\max},\ \forall n \in \mathcal{N}, \\
&\mathrm{C}_7: P_{u[n]} \le P_{\max},\ \forall n \in \mathcal{N},
\end{aligned} \tag{P1}$$

where $R_{k[n]}$ is the GN data rate which is given by

$$R_{k[n]} = \begin{cases} 0, & \gamma_{r,k[n]} < \gamma_{\rm thr} \\ B a_{k[n]} \log_2\left(1 + \gamma_{r,k[n]}\right), & \gamma_{r,k[n]} > \gamma_{\rm thr}, \end{cases} \tag{8}$$

where $\gamma_{\rm thr}$ is an SNR threshold. In more detail, C_1 forces the UAV trajectory to begin and end at the same point. In addition, C_2 indicates that the UAV speed $\upsilon_{[n]}$ cannot exceed the maximum UAV velocity $\upsilon_{\max}$, while C_3 defines that only one GN-BS pair can be served by the UAV-mounted FDR within a certain time slot. Moreover, C_4 indicates that the UAV's power consumption during its trajectory must not exceed its battery's available energy, while C_5 and C_6 set the lower and upper bounds for the optimization variables $\boldsymbol{a}, \boldsymbol{q}$, with C_6 ensuring the UAV remains within the predefined rectangular field. Lastly, C_7 describes that the UAV's transmission power should be less than $P_{\max}$, denoting the peak power limit of the UAV-mounted FDR.

B. Problem Solution

As it can be seen, problem (**P1**) is intractable since it contains both continuous and integer variables while its objective function is non-convex. To this end, a separation of the integer variable $\boldsymbol{A}$ and the continuous variable $\boldsymbol{Q}$ becomes essential. To address this, the alternate optimization technique is employed, which relies on successively optimizing each optimization variable block until convergence [4]. Therefore, for a fixed trajectory $\boldsymbol{Q}$ we have

$$\begin{aligned}
&\max_{\boldsymbol{A}} \min_{k} \left\{ \sum_{n=1}^{N} R_{k[n]} \right\} \\
\textbf{s.t}\ \ &\mathrm{C}_1: \sum_{k=1}^{K} a_{k[n]} \le 1,\ \forall n \in \mathcal{N}, \\
&\mathrm{C}_2: a_{k[n]} \in \{0,1\},\ \forall n \in \mathcal{N}.
\end{aligned} \tag{PA.1}$$

As it can be seen, problem (**PA.1**) is an integer programming problem, however, it is not in canonical form, since the

objective function is a non-linear function. Thus, by utilizing the auxiliary variable $r_{\min}$, (**PA.1**) is equivalently written as

$$\begin{aligned} \max_{\boldsymbol{A}, r_{\min}} \quad & r_{\min} \\ \text{s.t} \quad & \mathrm{C}_1: \sum_{k=1}^{K} a_{k[n]} \leq 1, \ \forall n \in \mathcal{N}, \\ & \mathrm{C}_2: a_{k[n]} \in \{0,1\}, \ \forall n \in \mathcal{N}, \\ & \mathrm{C}_3: \sum_{n=1}^{N} a_{k[n]} R_{k[n]} \geq r_{\min}, \ \forall k \in \mathcal{K}, \end{aligned} \tag{PA.2}$$

which is a mixed-integer linear programming problem, since for given trajectory $\boldsymbol{Q}$, $R_{k[n]}$ is constant. As a consequence, (**PA.2**) can be optimally.

Given the TDMA schedule $\boldsymbol{A}$, (**P1**) can be written as

$$\begin{aligned} \max_{\boldsymbol{x}_q, \boldsymbol{y}_q, r_{\min}} \quad & r_{\min} \\ \text{s.t} \quad & \mathrm{C}_1: \boldsymbol{q}_{[1]} = \boldsymbol{q}_{[N]}, \\ & \mathrm{C}_2: \upsilon_{[n]} \leq \upsilon_{\max}, \ \forall n \in \mathcal{N}, \\ & \mathrm{C}_3: B_c - \delta_t \sum_{n=1}^{N} P_{d[n]} \geq 0, \\ & \mathrm{C}_4: q_{\min} \leq \boldsymbol{q}_{[n]} \leq q_{\max}, \ \forall n \in \mathcal{N}, \\ & \mathrm{C}_5: P_{u[n]} \leq P_{\max}, \ \forall n \in \mathcal{N}, \\ & \mathrm{C}_6: \sum_{\substack{n=1, \\ a_{k[n]}=1}}^{N} R_{k[n]} \geq r_{\min}, \ \forall k \in \mathcal{K}, \end{aligned} \tag{PQ.1}$$

which is a non-convex problem due to the non-concave and dual branch objective function $R_{k[n]}$. Furthermore, in (7), $P_{[n]}$ is influenced by the UAV's speed $\upsilon_{[n]}$, which is derived from the differences in consecutive positions $x_{q[n]}$ and $y_{q[n]}$, thus, given that these positions are constants for each time slot, the relationship of $P_{d[n]}$ with x_q and y_q is affine. To tackle the non-convexity, we can convert $R_{k[n]}$ from a dual branch function into a single function by introducing an appropriate constraint that assures that the UAV always serves a GN for which the received SNR at the BS-side is above γ_{thr}. Additionally, $\forall n \in \mathcal{N}$ and $\forall k \in \mathcal{K}$ for which $a_{k[n]} = 1$, we can introduce the auxiliary variables $r_{k[n]}$, thus (**PQ.1**) can be rewritten as

$$\begin{aligned} \max_{\boldsymbol{x}_q, \boldsymbol{y}_q, r_{\min}, r_{k[n]}} \quad & r_{\min} \\ \text{s.t} \quad & (\textbf{PQ.1}): \mathrm{C}_1, \mathrm{C}_2, \mathrm{C}_3, \mathrm{C}_4, \mathrm{C}_5 \\ & \mathrm{C}_6: \sum_{\substack{n=1, \\ a_{k[n]}=1}}^{N} r_{k[n]} \geq r_{\min}, \ \forall k \in \mathcal{K} \\ & \mathrm{C}_7: \gamma_{r,k[n]} \geq \gamma_{\text{thr}}, \ \forall n \in \mathcal{N}, \ \forall k \in \mathcal{K} \text{ that } a_{k[n]} = 1, \\ & \mathrm{C}_8: R_{k[n]} \geq r_{k[n]}, \ \forall n \in \mathcal{N}, \ \forall k \in \mathcal{K} \text{ that } a_{k[n]} = 1. \end{aligned} \tag{PQ.2}$$

Considering the achievable rates of the examined network, the constraint C_7 can be equivalently written in a convex form as

$$\begin{aligned} \mathrm{C}_{7.A}: & \frac{(x_{q[n]} - x_k)^2 + (y_{q[n]} - y_k)^2 + {H_u}^2}{A_{1[n]}} \leq \frac{1}{\gamma_{\text{thr}}} \\ \mathrm{C}_{7.B}: & \frac{(x_{q[n]} - x_b)^2 + (y_{q[n]} - y_b)^2 + (H_u - H_{\text{BS}})^2}{A_{2[n]}} \leq \frac{1}{\gamma_{\text{thr}}}, \end{aligned} \tag{9}$$

where $\mathrm{A}_{1[n]} = \frac{P_t C_0 {d_0}^2 G_t A_r}{A_t G_r P_{u[n]} \omega + \sigma^2}$, and $\mathrm{A}_{2[n]} = \frac{A_t G_r P_{u[n]} C_0 {d_0}^2}{\sigma^2}$. Furthermore, by utilizing (5), and (6), and considering that the condition $\min\{x, y\} \geq t$ implies that both $x \geq t$ and $y \geq t$, thus C_8 in **PQ.3** can be equivalently divided into two separate constraints. Finally, the successive approximation method (SCA) is employed, thus, by substituting the non-convex terms with their first-order Taylor approximation, we formulate the convex optimization problem for the trajectory design in the examined scenario as follows:

$$\begin{aligned} \max_{\boldsymbol{x}_q, \boldsymbol{y}_q, r_{\min}, r_{k[n]}} \quad & r_{\min} \\ \text{s.t} \quad & (\textbf{PQ.2}): \mathrm{C}_1, \mathrm{C}_2, \mathrm{C}_3, \mathrm{C}_4, \mathrm{C}_5, \mathrm{C}_6, \mathrm{C}_{7.A}, \mathrm{C}_{7.B} \\ & \mathrm{C}_{8.A}: \frac{(x_{q[n]} - x_k)^2 + (y_{q[n]} - y_k)^2 + {H_u}^2}{A_{1[n]}} \\ & \quad - 2^{r_{k[n],0}} - (r_{k[n]} - r_{k[n],0}) 2^{r_{k[n],0}} \leq 0 \\ & \mathrm{C}_{8.B}: \frac{(x_{q[n]} - x_b)^2 + (y_{q[n]} - y_b)^2 + (H_u - H_{\text{BS}})^2}{A_{2[n]}} \\ & \quad - 2^{r_{k[n],0}} - (r_{k[n]} - r_{k[n],0}) 2^{r_{k[n],0}} \leq 0. \end{aligned} \tag{PQ.3-FDR}$$

As it can be observed, problem (**PQ.3-FDR**) is now convex, making it possible to be solved through standard optimization techniques like the interior-point method. The procedure for the joint TDMA-trajectory design is outlined in Algorithm 1. It is worth noting that the values for iter_1 and iter_2 are selected to ensure that the solutions from both the SCA and alternate optimization methods converge to a consistent solution, which is then presented as the final output of Algorithm 1.

Algorithm 1 Energy-Aware Trajectory Design for UAV-mounted FDR

```
Initialize iter_1, iter_2 B_c, δ_t, υ_max, U_w, D_w, R_{w,d}
for N = N_min, N_min + 1, ...., N_max do
    Initialize A_init, Q_init
    for i = 0, 1, 2, ..., iter_1 do
        For Q_init, solve (PA.2) and obtain A^i
        for j = 0, 1, 2, ..., iter_2 do
            For A^i, solve (PQ.3-FDR) and obtain Q^j
            r_{k[n],0} ← r^j_{k[n]}, s_{k[n],0} ← s^j_{k[n]}, t_{k[n],0} ← t^j_{k[n]}
        end for
        Q_init ← Q^{iter_2}
    end for
    Q* ← Q^{iter_2}
    For Q*, solve (PA.2) and obtain A*
end for
Obtain the best Q* and A*
```

IV. Simulation Results

In this section, we present numerical results to assess the performance of the proposed UAV-assisted network, whose power consumption and network parameters are detailed in Table I. Specifically, we consider an uplink communication system with a single-antenna BS located at the origin of this area, assisted by a UAV-mounted FDR serving 10 GNs whose transmit power is $P_t = 0$ dBm, that are distributed

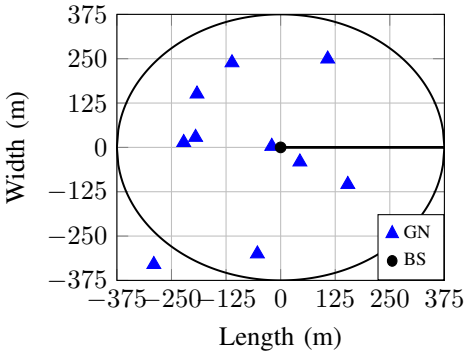

Fig. 1: Benchmark trajectory

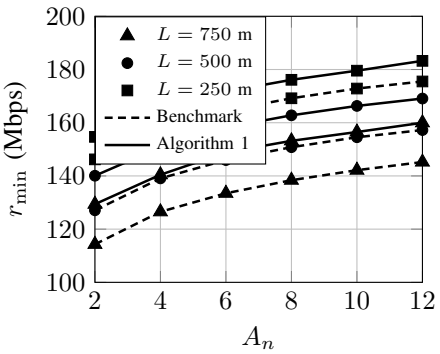

Fig. 2: Minimum rate versus FDR antennas for $\sigma^2 = -144$ dB

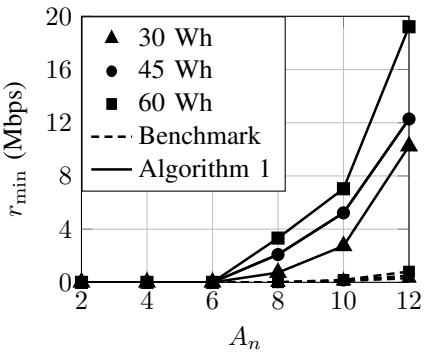

Fig. 3: Minimum rate versus FDR antennas for $\sigma^2 = -114$ dB

TABLE I: NETWORK PARAMETERS

Parameter	Notation	Value
UAV height	H_u	100 m
BS height	H_{BS}	15 m
Max transmit FDR power	$P_{\max}$	0 dBm
Time slot duration	δ_t	1 s
Reference distance	d_0	1 m
Bandwidth	B	1 MHz
Antenna gains	G_t, G_r	0 dB
Wavelength	λ	0.125 m
SIC coefficient	ω	-90 dB
Iterations	$\text{iter}_1, \text{iter}_2$	20, 20
UAV weight	U_{w}	3.25 kg
Antenna weight	A_{w}	8×10^{-3} kg
Battery weight	B_{w}	1.35 kg
Battery capacity	B_c	45 Wh
Inverse of pow. ampl. drain eff.	α	1.875
Transceiver consumption	P_R^C	1.5 W
Maximum achievable thrust	$T_{\max}$	17 kg
Maximum UAV speed	$v_{\max}$	62 km/h
Air density	ρ_a	1.225 kg/m^3
Air velocity	v_a	2.5 m/s (Light Air)
Drag shape coefficient	C_d	0.005@0°
UAV frame	A_{UAV}	0.5×0.5 m^2
Gravity acceleration	g	9.8 m/s^2
AT4130 KV230 T-MOTOR	C_1, C_2, C_3	10.5, -46, 744

randomly over a rectangular area with sides of $L = 750$ m, unless otherwise stated. Moreover, for the examined UAV frame which is capable of accommodating up to 12 antennas arranged as a ULA with an inter-distance of $\frac{\lambda}{2}$, we assume A_t and A_r to be equal. In addition, we adopt the circular trajectory of Fig. 1 as a benchmark, in which the UAV starts from the BS location, moves in a straight line to the midpoint on the right side of the field, follows a circle with radius $\frac{L}{2}$ centered at the axis origin, and finally retraces its path back to the origin. This benchmark trajectory is evaluated within the operational limits of the UAV's battery life, taking into account the trade-off between the trajectory size and the number of time slots available, under a TDMA scheduling scheme where each GN is served for $N_{\text{GN}} = \left\lfloor \frac{N}{K} \right\rfloor$. Finally, the results were calculated through Monte Carlo simulations with 1000 iterations.

Fig. 2 shows the effect of the number of the FDR antennas on $r_{\min}$, for $\sigma^2 = -144$ dB and $L = 750$ m, 500 m, and 250 m, respectively. As it can be seen, decreasing the value of L and increasing the number of FDR antennas enhances $r_{\min}$, with 12 antennas emerging as the optimal number for network performance. Furthermore, the application of Algorithm 1 further enhances the minimum rate, demonstrating its value in network performance improvement. Interestingly, Algorithm 1 identifies the hovering trajectory as the optimal approach for all the examined cases, which is a notable deviation from the expected optimization of the UAV-mounted FDR's path loss at intermediate distances between a GN and the BS. Specifically, the received SNR for the GNs consistently stays above γ_{thr} across all L values, influencing the trajectory design, as it leads to the conclusion that maximizing the flight duration, thus serving the GNs from the initial UAV position, is more advantageous than moving the UAV to each GN's optimal point, which results in the loss of time slots. Specifically, during the UAV's traversal to these optimal points, there would be instances where the UAV is not optimally positioned to serve any GN, leading to inefficient use of energy and further loss of time slots. To this end, the provided results underscore the practical implications of UAV-assisted networks, particularly emphasizing the balance between energy consumption and effective communication.

Fig. 3 showcases the influence of the FDR antennas on $r_{\min}$, comparing the outcomes from Algorithm 1 with those of the circular benchmark trajectory, under a scenario of increased noise power at -114 dB for an area with L equal to 750 meters, across different battery capacities. According to Fig. 3, for the case where $A_n \geq 8$, the optimized trajectory devised through Algorithm 1 significantly outperforms the benchmark scheme, affirming the critical role of TDMA scheduling and trajectory optimization in enhancing network performance. Additionally, Fig. 2 illustrates that higher battery capacities facilitate the UAV's ability to allocate more time slots for serving each GN, thus enabling longer service providing and more strategic UAV positioning. Consequently, increasing B_c not only extends the UAV's operational duration before battery depletion but also permits the execution of broader trajectories, optimizing the UAV's positioning across the field to serve GNs more effectively. Thus, Fig. 3 highlights the intricate relationship between battery capacity, number of antennas, and the strategic optimization of UAV trajectories in ensuring robust and efficient network performance, especially in scenarios affected by increased noise or cases with larger γ_{thr} values. Finally, the results in Fig. 3 contrast to the observations in Fig. 2, where un-

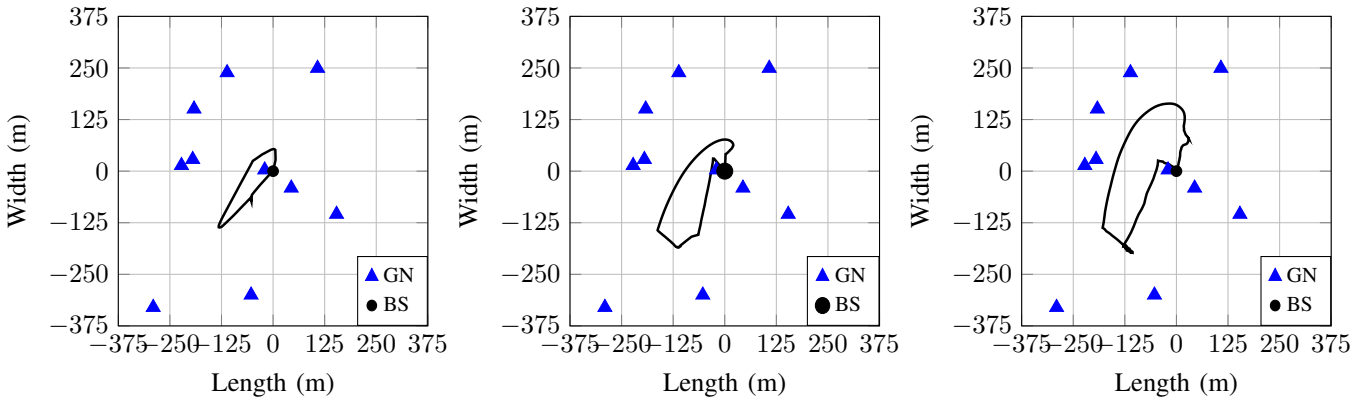

(a) $B_c = 30$ Wh (b) $B_c = 45$ Wh (c) $B_c = 60$ Wh

Fig. 4: Optimal UAV trajectories.

der lower noise levels, i.e., $\sigma^2 = -144$ dB, the UAV-mounted FDR prefers the hovering state, showcasing the adaptability of Algorithm 1 to varying environmental conditions and noise levels to optimize network performance.

Finally, Fig. 4 demonstrates the optimal trajectories for the UAV-mounted FDR system with 12 antennas across various battery capacities, illustrating how trajectories alter for different B_c values. As it can be seen, the different trajectory shapes for each B_c value reflect the relationship between battery capacity and the effectiveness of the UAV's flight path in enhancing network performance. In addition, each trajectory exhibits a distinctive spike in the bottom-left region for all analyzed B_c values, highlighting the strategic positioning required to service GNs that are located in this less favorable part of the rectangular area. In contrast, the right-hand side of the area, where GNs are sparser, necessitates fewer trajectory modifications. Thus, Fig. 4 underscores the significant impact of battery capacity on trajectory optimization, while signifying the adaptive design of the UAV trajectory to meet the unique demands of GN locations and distributions.

V. Conclusions

In this work, we thoroughly analyzed UAV-mounted FDR systems, focusing on the crucial integration of energy consumption models with trajectory optimization for viable UAV deployments. Specifically, we explored the UAV's operational demands versus flight duration, showing that strategic trajectory planning and energy dynamics consideration greatly improve network performance. Our approach confirmed the existence of an optimal UAV trajectory that balances operational requirements against energy limitations. Our optimization algorithm demonstrated the potential for optimizing network performance within these constraints. Additionally, our findings emphasized that the primary factor in UAV energy consumption is the motors, highlighting the necessity of considering energy efficiency in the design of UAV-mounted systems. Thus, our work underscores the need for energy-aware design of UAV trajectories, ensuring their feasibility in future network architectures.

Acknowledgment

This work has been funded by the European Union's Horizon 2020 research and innovation programs under grant agreement No 101139194 6G Trans-Continental Edge Learning.

References

[1] M. Giordani and M. Zorzi, "Non-terrestrial networks in the 6G era: Challenges and opportunities," *IEEE Netw.*, vol. 35, no. 2, pp. 244–251, 2021.

[2] P.-V. Mekikis, P. S. Bouzinis, N. A. Mitsiou, S. A. Tegos, D. Tyrovolas, V. K. Papanikolaou, and G. K. Karagiannidis, "Enabling wireless-powered IoT through incentive-based UAV swarm orchestration," *IEEE Open J. Commun. Soc*, vol. 4, pp. 2548–2560, 2023.

[3] Y. Zeng and R. Zhang, "Energy-efficient UAV communication with trajectory optimization," *IEEE Trans. Veh. Technol.*, vol. 16, no. 6, pp. 3747–3760, 2017.

[4] B. Li, S. Zhao, R. Zhang, and L. Yang, "Full-duplex UAV relaying for multiple user pairs," *IEEE Internet Things J.*, vol. 8, no. 6, pp. 4657–4667, 2021.

[5] N. V. Shende, O. Gürbüz, and E. Erkip, "Half-duplex or full-duplex communications: Degrees of freedom analysis under self-interference," *IEEE Trans. Wirel. Commun.*, vol. 17, no. 2, pp. 1081–1093, 2018.

[6] M. Hua, Y. Wang, Z. Zhang, C. Li, Y. Huang, and L. Yang, "Outage probability minimization for low-altitude UAV-enabled full-duplex mobile relaying systems," *China Commun.*, vol. 15, no. 5, pp. 9–24, 2018.

[7] D. De Paiva Mucin, D. P. M. Osorio, and E. E. B. Olivo, "Wireless-powered full-duplex UAV relay networks over FTR channels," *IEEE Open J. Commun. Soc.*, vol. 2, pp. 2205–2218, 2021.

[8] Z. Zhang, K. Long, A. V. Vasilakos, and L. Hanzo, "Full-duplex wireless communications: Challenges, solutions, and future research directions," *Proc. IEEE*, vol. 104, no. 7, pp. 1369–1409, 2016.

[9] L. Zhu, J. Zhang, Z. Xiao, X. Cao, X.-G. Xia, and R. Schober, "Millimeter-wave full-duplex uav relay: Joint positioning, beamforming, and power control," *IEEE J. Sel. Areas Commun.*, vol. 38, no. 9, pp. 2057–2073, 2020.

[10] P.-V. Mekikis and A. Antonopoulos, "Breaking the boundaries of aerial networks with charging stations," in *Proc. IEEE International Conference on Communications (ICC)*, 2019, pp. 1–6.

[11] Y. Xiao, D. Tyrovolas, S. A. Tegos, P. D. Diamantoulakis, Z. Ma, L. Hao, and G. K. Karagiannidis, "Solar powered UAV-mounted RIS networks," *IEEE Commun. Lett.*, vol. 27, no. 6, pp. 1565–1569, 2023.

[12] A. Talebi and W. A. Krzymien, "Multiple-antenna multiple-relay cooperative communication system with beamforming," in *Proc. IEEE Vehicular Technology Conference*, 2008, pp. 2350–2354.

[13] J. Ma, C. Huang, and Q. Li, "Energy efficiency of full- and half-duplex decode-and-forward relay channels," *IEEE Internet Things J.*, vol. 9, no. 12, pp. 9730–9748, 2022.

[14] D. Tyrovolas, P.-V. Mekikis, S. A. Tegos, P. D. Diamantoulakis, C. K. Liaskos, and G. K. Karagiannidis, "Energy-aware design of UAV-mounted RIS networks for IoT data collection," *IEEE Trans. Commun.*, vol. 71, no. 2, pp. 1168–1178, 2023.